Nuclear Instruments and Methods in Physics Research B 267 (2009) 1264–1268

Contents lists available at ScienceDirect

Nuclear Instruments and Methods in Physics Research B

journal homepage: www.elsevier.com/locate/nimb

Mechanisms of ion-induced GaN thin layer splitting

O. Moutanabbir [a,*], Y.J. Chabal [b], M. Chicoine [c], S. Christiansen [a], R. Krause-Rehberg [d], F. Schiettekatte [c], R. Scholz [a], O. Seitz [b], S. Senz [a], F. Süßkraut [d], U. Gösele [a]

[a] Max Planck Institute of Microstructure Physics, Weinberg 2, Halle (Saale) 06120, Germany
[b] Department of Materials Science, University of Texas at Dallas, 800 West Campbell Road Richardson, TX 75080, United States
[c] Département de Physique, Université de Montréal, Succursale Centre Ville, Montréal (Québec), Canada H3T 1J4
[d] Martin-Luther-University Halle-Wittenberg, Friedemann-Bach-Platz 6, Halle (Saale) 06108, Germany

ARTICLE INFO

Article history:
Available online 18 February 2009

PACS:
61.80.Jh
61.82.Fk
61.72.uj
61.72.Qq
61.72.J–

Keywords:
GaN
Ion-cut
Ion implantation
Blistering
Voids
Vacancy complexes

ABSTRACT

The underlying physics and the role of H-defect interaction in H ion-induced splitting of GaN were investigated by transmission electron microscopy, high resolution X-ray diffraction, positron annihilation spectroscopy, ion channeling, elastic recoil detection, and infrared spectroscopy. A high concentration of void-like nanoscopic structures, nanobubbles, is detected immediately after implantation. Positron annihilation measurements demonstrate that the detected structures are vacancy clusters. FTIR data show that H-defect vibrational spectrum peaks at 3141 cm^{-1} mode attributed to V_{Ga}–H_4. A large fraction of H was found to be trapped in higher frequency modes which we associate tentatively to N–H stretch modes in the internal surfaces of nanobubbles. These nanobubbles persist during annealing up to 450 °C. An increase of the strain is observed in this temperature range. This strain relaxes partially above 450 °C following the formation of the platelets which are embryos of the microcracks.

1. Introduction

In a technological context characterized by the urgent need for environment compatible energy resources, light-emitting diode (LED) solid-state lighting emerges as one of the strategies to achieve the reduction of greenhouse gas emissions and energy consumption. GaN and related materials heterostructures have been the building blocks of LED-based devices [1]. These heterostructures provide also a wide spectrum of applications in data communications, sensing, optoelectronics, and biophotonics. However, these emerging technologies perform far below their full potential due to the limited quality of the heteroepitaxial structures. Indeed, GaN used in device fabrication is grown epitaxially on sapphire despite its poor lattice and thermal match to GaN. The densities of misfit and threading dislocations in GaN layers deposited on sapphire range typically from 10^8 to 10^{10} cm^{-2} whereby the efficiency of GaN devices is limited. High quality GaN bulk substrates can be produced by hydride vapor phase epitaxy growth of thick GaN layers on sapphire and subsequent separation from the sapphire substrate. The current cost of these freestanding (fs–)GaN wafers is still exceedingly high, which makes the concept of transfer of many thin layers from one fs–GaN wafer to appropriate host substrates technologically and economically highly attractive. A promising process to transfer bulk quality sub-micrometer-thin layers onto a foreign material without any epitaxial relationship to be required between layer and substrate is the transfer by direct wafer bonding and hydrogen (H) implantation induced ion-cutting [2]. This process has been successfully applied to various semiconductor materials leading to a variety of high quality heterostructures frequently unattainable by epitaxy. Independently of the material, the interaction of the implanted species with the radiation damage seems to play the key role in the splitting process. Silicon has been subject of intensive investigations [3], however, only few works were devoted to study the basic mechanisms of ion-induced splitting of other semiconductors [4–6]. GaN exfoliation induced by H implantation was first reported by Kucheyev et al. [7]. However, detailed investigations of the underlying physics of ion slicing of GaN are still in their infancy [8]. In this work, we combine a variety of experimental techniques to identify some of the atomic processes and structural transformations involved in H ion-induced fs–GaN splitting. Understanding these basic mechanisms is vital for a better control of the ion-cut technology.

* Corresponding author. Fax: +49 345 551 1223.
E-mail address: moutanab@mpi-halle.mpg.de (O. Moutanabbir).

0168-583X/$ - see front matter © 2009 Elsevier B.V. All rights reserved.
doi:10.1016/j.nimb.2009.01.028

2. Experimental details

Our experiments were carried out using LED quality fs–GaN. ~300 μm-thick 2-inch double side polished undoped fs–GaN wafers were subject to room temperature (RT) H implantation at 50 keV with a fluence of 2.6×10^{17} atom/cm^2. Different techniques were used to characterize the implantation damage in as-implanted and annealed substrates. The morphology of the implanted region was observed by cross-sectional transmission electron microscopy (XTEM) using a Philips CM 20T machine operated at 200 kV. In order to assess the lattice disorder, high resolution X-ray diffraction (HRXRD) measurements were carried out using a Philips X'Pert MRD system with Cu Kα radiation. Rutherford backscattering in channeling mode (RBS/C) was used to characterize the implantation-related displacements and lattice distortion in the implanted samples. RBS/C measurements along the [0001] axis of GaN were performed using 2 MeV $^+$He beam on the Tanderton accelerator at the Université de Montréal. Measurements were also carried out using an unimplanted wafer (virgin). Using the same setup, with different detection geometry, H depth profile was measured by elastic recoil detection (ERD). The H-defect local vibrational modes were acquired using Fourier transform infrared (FTIR) in a Thermo-Nicolet spectrometer using a liquid nitrogen cooled mercury cadmium telluride detector with a low frequency cutoff near 600 cm^{-1}. Positron annihilation spectroscopy (PAS) was used to characterize the implantation-induced vacancy clusters and voids. Positron beam measurements were done with the POSSY system at Martin-Luther University [9, p. 31]. Positrons of a 20 mCi 22-Na source are moderated to form a monoenergetic positron beam by a tungsten single crystal foil. The positrons are implanted into the GaN samples with energies from 0.2 to 30 keV, corresponding to a mean penetration depth up to 1.5 μm. Because this beam is continuous, Doppler broadening spectroscopy is applied to study the defect depth profile of the implanted samples. As a result of these measurements the *S* parameter was determined [9, p. 18]. The *S* parameter is defined as the area of the central part of the annihilation line at 511 keV divided by the area of the whole gamma line after background subtraction. The *S* parameter increases when positrons are trapped in open-volume defects. However, the amount of the increase depends on both the size of the defects (mono-, divacancies or small vacancy clusters) and their concentration.

3. Results and discussion

During the implantation of energetic H ions into GaN several physical and chemical processes take place leading to a variety of damage related structures including point defects in both sublattices, H-defect complexes, point defects clusters, and free hydrogen. Fig. 1 displays H and atomic displacement depth profiles in as-implanted GaN as deduced from ERD and ion channeling analyses, respectively. The data show that the H profile is peaked at ~320 nm with a variance of about 100 nm in agreement with SRIM calculations [10]. The H concentration at the peak is found to be $\sim 1.2 \times 10^{22}$ H/cm^3 corresponding to an atomic concentration of about ~13% which is ~3–5 times higher than the concentration needed for silicon exfoliation [3]. RBS/C analysis shows that the atomic displacement distribution reaches a maximum of ~27% at a shallower depth of ~285 nm [11]. The displacement profile is obtained by subtracting the unimplanted ion channeling spectrum from the implanted one. The two-bean model was then employed to deconvolute the dechanneling [12]. The program *Allegria* was used to process the signal and convert it to atomic displacements depth distribution [13]. By assuming that the dechanneling originates from direct scattering of He ion on Ga interstitials, we estimate the displacements per ion to be ~2.5, much smaller than ~10 calculated at lattice temperature of 0 K in the absence of the dynamic annealing [10]. This indicates that about ~75% or more of Frenkel pairs recombine during the implantation process. This remains a very simple estimation given the complexity of the microstructure contributing to the dechanneling signal. This approximate annihilation rate is relatively smaller than in the case of Si implanted under ion-cut conditions (~>90%) [3]. Therefore, the dynamic annealing cannot explain the unusually high fluence required for the splitting of GaN. The nature of H-defect complexes, their thermal evolution, and point defects diffusivities may play the most critical role than the absolute amount of the surviving defects.

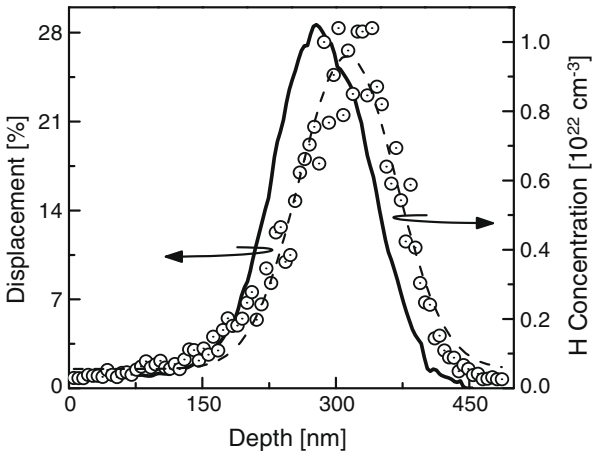

Fig. 1. Implantation damage and *H* concentration depth profiles as deduced from ion channeling and ERD, respectively.

Typical HRXRD spectra of GaN before and after H implantation are presented in Fig. 2. We notice that H implantation creates a significant out-of-plane tensile strain which is detectable as a broadening at the left side of the (0002) GaN diffraction peak. Post-implantation wafer curvature measurement indicates that this out-of-plane tensile strain is accompanying an in-plane biaxial compressive stress [14]. Close examination shows that the as-implanted diffraction spectrum consists of two different features shifted by about 0.015 and ~0.14 degree from the (0002) diffraction peak (Fig. 2). These two features reveal that the implantation damage induces two distinct strained regions. The highly strained region is characterized by a relatively broad peak. We attribute this peak to a highly defective zone. Such a defective zone can be seen

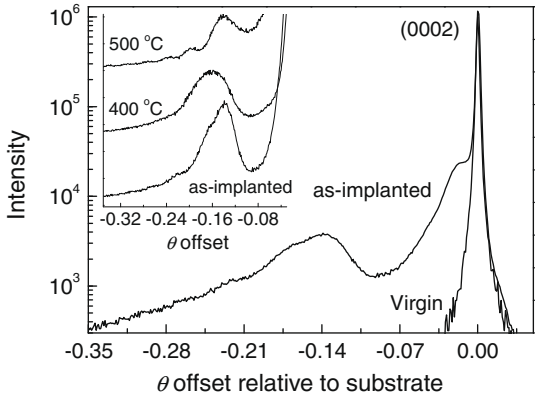

Fig. 2. HRXRD ω–2 scans of (0002) GaN before and after H implantation. Inset: evolution of damage-induced strain after annealing at 400 °C and at 500 °C (the intensities are given in linear scale).

in Fig. 3 showing a XTEM micrograph of the as-implanted sample. We note that H ion implantation induces broad damage band extending over a 300 nm-thick layer starting about 200 nm below the surface. No extended defects are observed at the implanted fluence. High magnification image of the implanted zone taken under focus (inset) indicates the presence of a high density of nanoscopic bright spots of ~1–2 nm in diameter. The change in their contrast during focus variation suggests that they are void-like structures. This observation is supported by Doppler broadening *S* parameter depth profile measurements (Fig. 4). Indeed, in the implanted region an enhancement of the *S* parameter of 6.5% is observed indicating the presence of open volume defects which support the XTEM observations. Such an increase is too large to be caused by monovacancies (the maximum increase expected for mono- or divacancies is smaller than 3%). Thus, we conclude that positrons are trapped by small vacancy clusters. The size of these clusters can only be determined by positron lifetime experiments. Data from such an experiment will be described in a forthcoming paper.

Fig. 5 displays the FTIR spectrum of H-implanted GaN recorded at room temperature. The spectrum reveals a broad, asymmetric band in the absorption spectrum in the wavenumber range 3000–3400 cm^{-1}. No IR absorption signal is detected from unplanted GaN in this range. These frequencies appear to be associated with N–H stretch modes of Ga-vacancy (V_{Ga}) defects decorated with one or several H atoms (V_{Ga}–H_n) [15]. The H attachment to dangling bonds stabilizes the vacancies and small clusters and prevents their dynamic annihilation. No N-vacancy related modes are detected under our conditions. The observed broadband is characterized by three distinct bumps or shoulders at ~3060, ~3141, and ~3200 cm^{-1}. Ga has two stable isotopes ^{69}Ga and ^{71}Ga with natural abundances of 60.1 and 39.9%, respectively. This gives three possible isotopic variations of N–H modes with Ga backbonds. However, given the small variation in the reduced mass between the two isotopes, we can rule out the possibility that the three isotopic configurations would produce the observed shoulders. Thus, we conclude that the features in the IR spectrum originate from H distribution among several modes with different atomic and structural properties. It is worth pointing out that the implantation of a very low fluence gives rise to several clear and narrow peaks at frequencies in the range of 3020 to 3140 cm^{-1} [15,16]. The dominant feature in our spectrum 3141 cm^{-1} is close to the mode 3139.5 cm^{-1} attributed to V_{Ga}–H_4 [15]. However, the absence of clear peaks in our data is indicative of a high lattice disorder induced by the implantation under ion-cut conditions. Moreover, the detected N–H stretch modes (Fig. 5) are shifted to higher

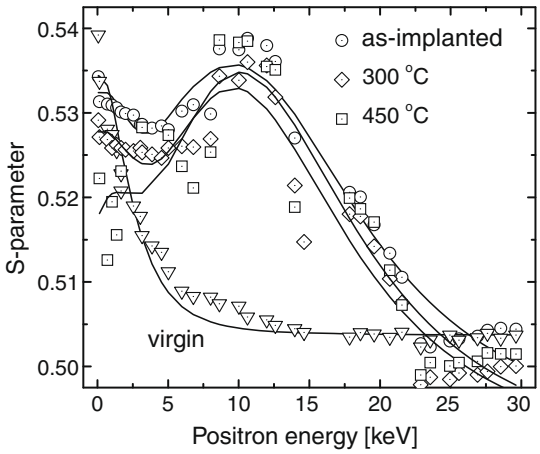

Fig. 4. *S* parameter depth profiles of GaN: virgin (triangle), as-implanted (circles), annealed at 300 °C (rhombus), and at 450 °C (square).

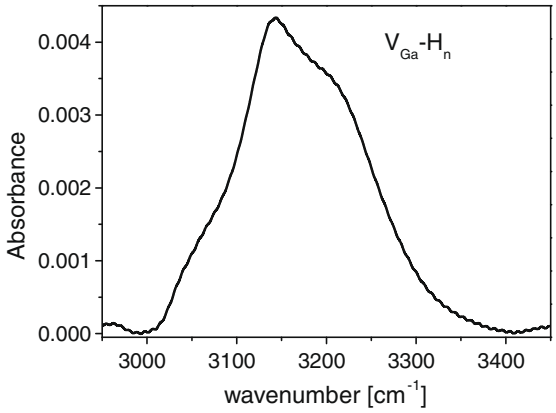

Fig. 5. Vibrational spectrum measured at RT of H-implanted GaN at a fluence of 2.6×10^{17} cm^{-2}.

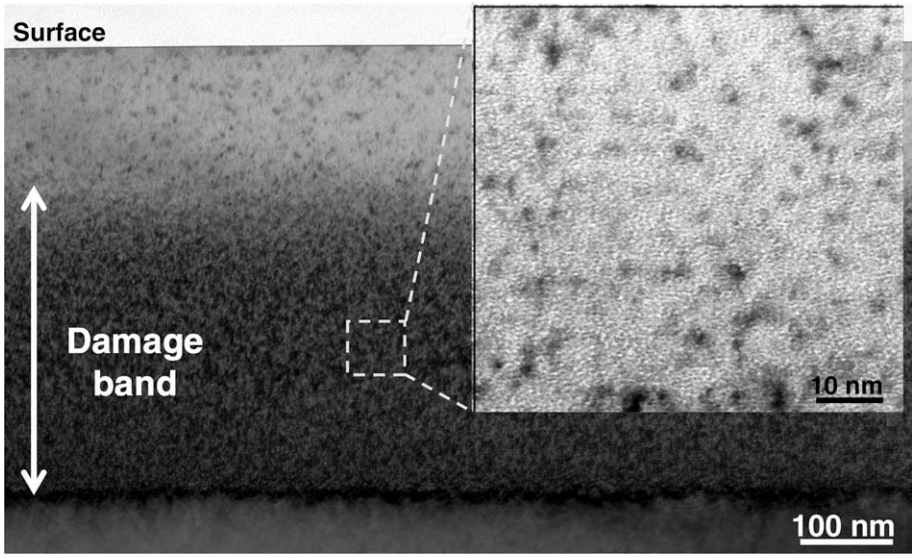

Fig. 3. XTEM image of 50 keV H-implanted GaN at a fluence of 2.6×10^{17} cm^{-2}. Inset: High magnification image of a selected area in the damage band.

frequencies by ~260 cm^{-1} compared to data in Ref. [13]. Similar observations can be drawn from parallel systems, such as H-implanted silicon in which H-defect vibrational modes overlap in a broadband which shifts to higher frequencies by increasing the implantation fluence [17]. Additionally, the steric interaction with H_2 gas can also induce a shift in stretching modes frequency [18]. Based on these studies it is tempting to assign the high frequency modes ($k > 3140$ cm^{-1}) to H trapped in internal surfaces of implantation induced nanobubbles. Presumably these surfaces bound modes have the largest effective spring constant because of the lack of restoring forces from surrounding atoms other than the one involved in the principle bond. Similar conclusions were made by Seager et al. who attributed the 3190 and 3210 cm^{-1} modes to mono- and dihydride species bonded to $\{10\bar{1}1\}$-like planes forming the large hexagonal cavities induced by H implantation at excessively high fluences [19].

Thermoevolution of H-induced damage is investigated next. In Fig. 6 we show a representative set of XTEM images. We note that annealing up to 450 °C does not trigger any significant morphological changes in the damage band (Fig. 6(a)). Similarly to the as-implanted sample, the implanted zone remains decorated with nanobubbles. In the course of the annealing up to 450 °C no further clustering nor healing of the defects are observed in Doppler broadening measurements (Fig. 4). Only the surface-*S* parameter changes ($E < 3$ keV) indicating a chemical or structural change in the outermost layer of the substrate. This absence of vacancy clustering in this temperature range indicates that the necessary voids for splitting assemble dynamically during the implantation process. This behavior differs completely from the evolution observed in Si where an important increase of void-like defects was found to precede the exfoliation [20,21]. Interestingly, at this temperature range the low-strain shoulder in X-ray diffraction spectra (not shown) vanishes, whereas the high-strain band downshifts indicating a further increase in the strain (Fig. 2 (inset)). A small increase in temperature to 500 °C leads to the formation of platelet-like nanoscopic cracks parallel to the surface (Fig. 6(b)). Further increase in the annealing temperature to 600 °C induces large cracks leading to a complete exfoliation of a ~340 nm-thick layer (Fig. 6(c)). Our detailed XTEM data show that transition from nanobubbles to platelets to microcracks occurs within a temperature window as narrow as 25 and 50 °C, respectively. It is worth pointing out that the platelets do not result from the coalescence of nanobubbles. Presumably stress-induced Ga–N bond breaking could be the origin of the formation of these platelets. As mentioned above, X-ray data suggested a buildup of strain prior to the formation of the platelets in agreement with recent ion channeling observations [8]. The origin of this strain enhancement was attributed to a combined influence of the highly pressurized nanobubbles and self-interstitial clusters which can increase the in-plane compressive strain causing a strong lattice distortion [8]. This process will ultimately lead to a weakening of the atomic bonding. The system attains criticality around 450 °C. The Ga–N bond breaking would be an efficient path for the relaxation of the internal strain. Indeed, higher temperature X-ray diffraction spectra (Fig. 2 (inset)) provide evidence for a relief of the strain following the formation of platelets. These platelets define the

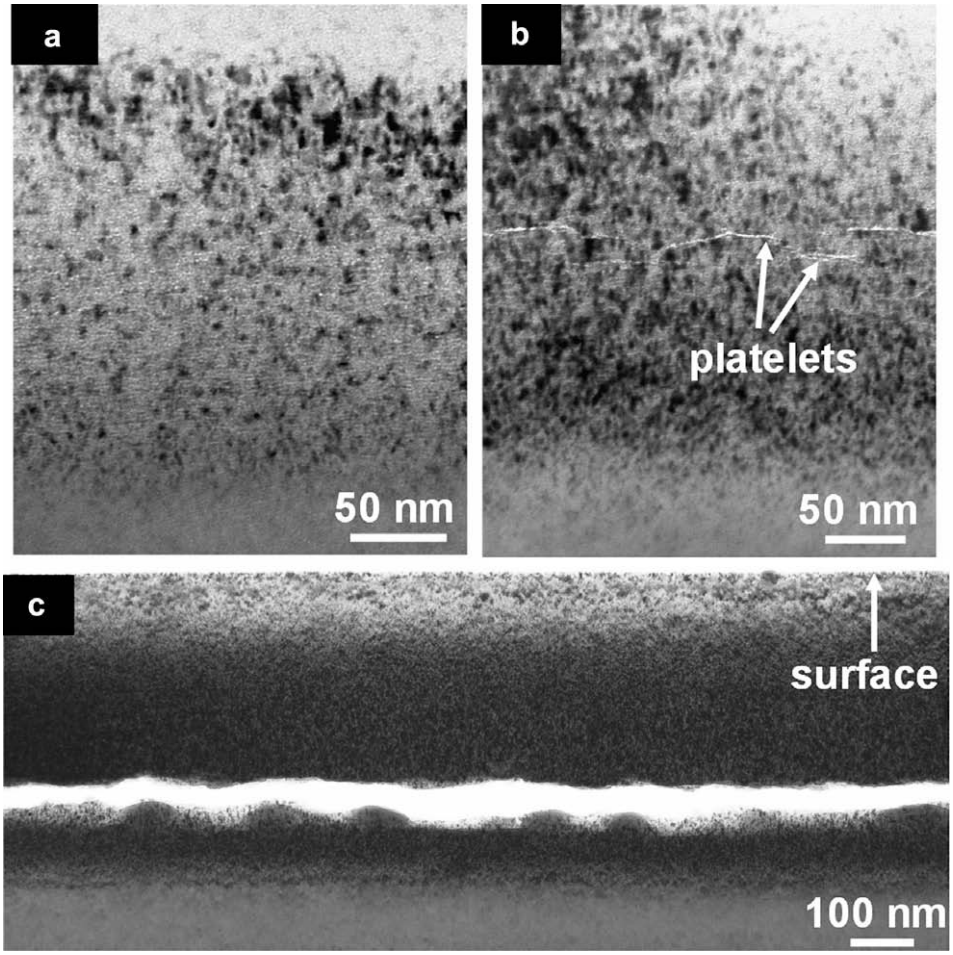

Fig. 6. XTEM micrographs of H-implanted GaN annealed at different temperatures: 450 °C (a), 500 °C (b), and 600 °C (c).

fracture paths for the exfoliation. Finally, despite that H_2 is believed to play a crucial role in internal pressure buildup, probing and understanding its exact thermal behavior in GaN under ion-cut conditions will remain an open challenge as it is still for Si [3]. The only available data from first-principles calculations suggest that H_2 in GaN requires unfavorably high formation energy ($\sim$2.4 eV in vacuum) compared to Si [22]. This could explain in part the high fluence needed for GaN ion-cutting.

4. Conclusion

To conclude, we investigated the critical transformations involved in the splitting of GaN by H implantation and subsequent annealing. We found that vacancy clustering during the implantation process leads to the assembly of 1–2 nm nanobubbles. H is suggested to chemically stabilize these vacancy clusters. A large fraction of H was found to be trapped in high frequency modes which we associate tentatively to N–H stretch modes in the internal surfaces of nanobubbles. These nanobubbles persist during annealing up to 450 °C. No further agglomeration of vacancies and growth of void-like structures are detected in this range of temperature, whereas the radiation-induced strain was found to increase. Annealing above this temperature leads to the formation of platelets parallel to the surface, inducing a relaxation of the internal strain. At higher temperature, the platelets evolve into extended internal surfaces leading to the exfoliation of a thin layer.

Acknowledgment

We are thankful to S. Hope for the help with TEM preparation. This work was supported in part by the German Federal Ministry of Education and Research BMBF (Contract No. 01BU0624: CrysGaN).

References

[1] G.F. Neumark, I.L. Kuskovsky, H. Jiang, Wide bandgap light-emitting materials and devices, Wiley-VCH, 2007.
[2] M. Bruel, Electron. Lett. 31 (1995) 1201.
[3] B. Terreault, Phys. Stat. Sol. (A) 204 (2007) 2129.
[4] A. Fontcuberta, I. Morral, J.M. Zahler, M.J. Griggs, H.A. Atwater, Y.J. Chabal, Phys. Rev. B 72 (2005) 085219.
[5] J.M. Zahler, A. Fontcuberta, I. Morral, M.J. Griggs, H.A. Atwater, Y.J. Chabal, Phys. Rev. B 75 (2007) 035309.
[6] N. Desrosiers, A. Giguère, B. Terreault, M. Chicoine, F. Schiettekatte, Nucl. Instr. and Meth. B 266 (2008) 1880.
[7] S.O. Kucheyev, J.S. Williams, C. Jagadish, J. Zou, G. Li, J. Appl. Phys. 91 (2001) 3928.
[8] O. Moutanabbir, R. Scholz, S. Senz, U. Gösele, M. Chicoine, F. Schiettekatte, F. Süßkraut, R. Krause-Rehberg, Appl. Phys. Lett. 93 (2008) 031916.
[9] R. Krause-Rehberg, H.S. Leipner, Positron Annihilation in Semiconductors, Springer-Verlag, Berlin, 1999.
[10] J.F. Ziegler, J.B. Biersack, U. Littmark, The Stopping and Range of Ions in Solids, Pergamon, New York, 1985 <http://www.srim.org>.
[11] The calculation of an exact depth scale requires an iterative procedure since the channeled and dechanneled ions suffer different energy losses.
[12] M. Bianconi, G. Lulli, F. Spallacci, E. Albertazzi, R. Nipoti, A. Carnera, C. Cellini, Nucl. Inst. and Meth. B 122 (1997) 689.
[13] F. Schiettekatte, M. Chicoine, S. Gujrathi, P. Wei, K. Oxorn, Nucl. Inst. and Meth. B 219–220 (2004) 125.
[14] O. Moutanabbir, S. Senz, R. Scholz, S. Christiansen, M. Reiche, A. Avramescu, U. Strauss, U. Gösele, Electrochem. Solid State Lett. 12 (2009) H105.
[15] M.G. Weinstein, C.Y. Song, M. Stavola, S.J. Pearton, R.G. Wilson, R.J. Shul, K.P. Killeen, M.J. Ludowise, Appl. Phys. Lett. 72 (1998) 1703.
[16] R.N. Pereira, B. Bech Nielsen, M. Stavola, M. Sanati, S.K. Estreicher, M. Mizuta, Physica B 376–377 (2006) 464.
[17] O. Moutanabbir, B. Terreault, M. Chicoine, F. Schiettekatte, Appl. Phys. A 80 (2005) 1455.
[18] Y.J. Chabal, M.K. Weldon, Y. Caudano, B.B. Stefanov, K. Raghavachari, Physica B 273–274 (1999) 152.
[19] C.H. Seager, S.M. Myers, G.A. Peterson, J. Han, T. Headley, J. Appl. Phys. 85 (1999) 2568.
[20] O. Moutanabbir, B. Terreault, M. Chicoine, F. Schiettekatte, P.J. Simpson, Phys. Rev. B 75 (2007) 075201.
[21] P.J. Simpson, A.P. Knights, M. Chicoine, K. Dudeck, O. Moutanabbir, S. Ruffel, F. Schiettekatte, B. Terreault, Appl. Surf. Sci. 255 (2008) 63.
[22] J. Neugebauer, C.G. Van de Walle, Phys. Rev. Lett. 75 (1995) 4452.